

Statistical atmospheric inversion of local gas emissions by coupling the tracer release technique and local scale transport modelling: a test case with controlled methane emissions

Sébastien Ars¹, Grégoire Broquet¹, Camille Yver Kwok¹, Yelva Roustan², Lin Wu¹, Emmanuel Arzoumanian¹, and Philippe Bousquet¹

¹Laboratoire des sciences du climat et de l'environnement (LSCE/IPSL), CNRS-CEA-UVSQ, Université de Paris-Saclay, Centre d'Études Orme des Merisiers, Gif-sur-Yvette, France

²CEREA, Joint Laboratory École des Ponts ParisTech / EDF R&D, Université Paris-Est, Champs-sur-Marne, France

Abstract

This study presents a new concept for estimating the pollutant emission rates of a site and its main facilities using a series of atmospheric measurements across the pollutant plumes. This approach is based on a combination of the tracer release method, a local scale atmospheric transport model and a statistical atmospheric inversion approach. The conversion between the tracer controlled emission and the measured tracer atmospheric concentrations across the plume provides knowledge on the atmospheric transport. The concept of the method consists of using this knowledge to optimize the configuration of the transport model parameters and the model uncertainty statistics in the inversion system. The pollutant rates of each source are then inverted to optimize the match between the concentrations simulated with the transport model and the pollutants' measured atmospheric concentrations, accounting for the transport model uncertainty. The potential of the concept is evaluated with a relatively simple implementation based on a Gaussian plume model and a series of inversions of controlled methane point sources using acetylene as a tracer gas. The experimental conditions are chosen so that the use of a Gaussian plume model to simulate the atmospheric transport is relevant. In these experiments, different configurations of methane and acetylene point source locations are tested to assess the efficiency of this method in comparison with the classic tracer release technique to cope with the distances between the different methane and acetylene sources. The results from these controlled experiments demonstrate that when the targeted and tracer gases are not well collocated, this new approach provides a better estimate of the emission rates than the tracer release technique. As an example, the relative error between the estimated and actual emission rates is reduced from 32% with the tracer release technique to 16% with the combined approach in the case of a tracer located 60 metres upwind of a single methane source. This method also enables the estimation of the different sources within a same site. This evaluation demonstrates the potential of the new concept proposed in this study to provide better estimates than the traditional tracer release technique. However, further studies and more complex implementations will be required to generalise its applicability and strengthen its robustness.

1 Introduction

Atmospheric pollution due to anthropogenic activities is a major issue both for air quality and for climate change because of the increase in the atmospheric concentrations of greenhouse gases. Industrial sites are known to emit a significant part of the pollutants and greenhouse gases. For instance in France, industrial

emissions represent between 10 and 30% of major air pollutants, such as carbon and nitrous oxides (Bort and Langeron, 2016). Currently, industries must list their emissions through national inventory reports, and some of them commit to reducing these emissions. However, the choice of an appropriate mitigation policy and the verification of its results require a good understanding of the emitting processes and a precise quantification of the emission rates. Industrial emissions are difficult to model and quantify because of the diversity and the time variability of the emitting processes. Many emitting industrial sites have a typical size of 100–500 m², and they emit pollutants from very specific locations within this area. The transport of these pollutants in the atmosphere over distances from 0.1 to several kilometres from such sites can be viewed as a plume from point sources. One approach developed to quantify the emissions from such sites involves atmospheric concentration measurements around the site, particularly across these emission plumes, and proxies of the atmospheric transport. These proxies are used to characterise the link between the emission rate and the structure and amplitude of the emission plume. The “inversion” of this link enables the estimate of the emission rates from the observed concentrations. Among the different techniques to estimate emissions from concentrations is the tracer release method. It is based on mobile continuous measurements across the emission plumes of the studied pollutant and of a tracer purposely emitted as close as possible to the pollutant source with a known rate (Lamb et al., 1995). In this method, the proxy of the atmospheric transport is given by the relation between the tracer emission and the tracer concentrations. In practice, it provides estimates of the emissions of a site over a relatively short time window, i.e., typically few hours during a given day, which corresponds to the time during which the tracer can be released and mobile measurement can be conducted.

This approach is relatively simple to implement and enables instantaneous estimations for a large number of sites. Nevertheless, this technique encounters some limitations, particularly (i) when it is difficult to position the tracer emission close to the sources, (ii) when the sources are spread over a significant area compared with the distance between the sources and the location of the measured concentrations, or (iii) when targeting individual estimates of the different emission rates from multiple sources whose plumes overlap over a given site (Mønster et al., 2014; Roscioli et al., 2015).

Typically, in industrial sites, pollutant sources may be sporadic and diffusive over a large area, their location can be difficult to reach and the spatial distribution of the emissions is not always precisely known, e.g., when considering transitory leakages or widespread and heterogeneous sources. In these cases, the tracer release method can induce errors in the flux estimation since the tracer plume by itself cannot be used as an accurate proxy of the local transport from the targeted gas sources to the measurement locations. Moreover, this approach can hardly be used to provide an estimate of the different sources within a site.

Other techniques exploit atmospheric measurements using local atmospheric dispersion models to simulate the transport of the targeted gas from its sources to the measurement locations (Lushi and Stockie, 2010). In theory, the model and the inversion of this proxy of the atmospheric transport can be applied for a point source or for a source whose spread is known. In principle, they can also be applied to multiple sources. The principle of this technique is relatively simple, but the representation of the emission spread in these models, and the separation of the different plumes associated with the different sources when targeting multiple sources can bear large uncertainties. In particular, the transport over short distances or time scales in a complex terrain can be characterised by complex turbulent structures which are difficult to match with a model even when the underlying processes are taken into account. Moreover, when targeting several sources, the mathematical inversion of the transport from the sources to the measurements artificially requires extending or limiting the number of data extracted from the measurements to the number of sources to be quantified. It can lead to a loss of information or it can hide the fact that the problem is underconstrained when the plumes overlap too much.

Accounting for uncertainties in the model and addressing under- or overconstrained mathematical problems when using the correct number of data that corresponds to the complementary pieces of information in the measurements can be addressed using a statistical inversion framework, which can be viewed as a generalised inversion technique. In such a framework, a statistical estimate of the emission rates for the different targeted sources is derived to optimize the fit to the measurements, accounting for the statistical uncertainties in the source and transport modelling, in the measurements and in the prior knowledge about the source location and magnitude (Goyal et al., 2005). Statistical inversions using atmospheric transport models and atmospheric concentration measurements have been used for decades to infer surface sinks and/or sources of pollutants and greenhouse gases at the continental to the city scales (Gurney et al., 2003; Bréon et al., 2015). However, the skill of such approaches strongly relies on

a good accuracy of the modelling of the transport and of the emission spatial distribution, and on the ability to characterise the statistics of modelling uncertainties.

This study describes a concept of combination between the tracer release technique, local scale transport modelling and the statistical inversion framework to improve the estimation of gas emissions from one or several point sources in an industrial site-scale configuration. Based on the same measurement framework as the tracer release technique, the concept consists of using the knowledge on the transport given by the tracer controlled emission and concentration measurements across the emission plumes to optimize the calibration of the transport model parameters and to assess the statistics of the model errors for the configuration of the inversion system. A practical implementation with a Gaussian plume model is proposed and its robustness is evaluated to illustrate the principle and the potential of our general the concept. This practical implementation is tested for the quantification of methane emissions during a time window of several hours using acetylene as a tracer gas and mobile measurements across the methane and acetylene. Methane is an important greenhouse gas with largely unknown point source emissions (Saunio et al., 2016). Typical methane emitting sites due to anthropogenic activities include waste processing plants (wastewater treatment plants and landfills), oil and gas extraction and compressing sites and farms (Czepiel et al., 1996; Yver Kwok et al., 2015; Marik and Levin, 1996).

Such sites contain widespread and heterogeneous sources (like the basins in waste water treatment plants, the cells in landfills and the livestock in farms) and are prone to fugitive leakages (especially in the oil and gas sectors). Until recently, there was no strong incentives to report emissions and when reported, they were usually derived using standard bottom-up product of emission factors times quantity of waste/wastewater/gas processed and/or relatively simple emission models (IPCC, 2013). However, a precise estimate of the methane emissions from such sites based on atmospheric techniques could help their operators in their local action plans to mitigate their emissions in the context of climate change. While a continuous monitoring of such emissions would help characterise the dependence of such emissions on meteorological conditions and on the change in the site processes through time, instantaneous estimates of the emissions through a dedicated measurement campaign can help to detect and provide a useful order of magnitude for such sources that are generally poorly known (Yver Kwok et al., 2015). Finally, the results from series of campaigns can be extrapolated into estimates for longer timescales.

Here, we conduct a series of controlled experiments with known emissions of methane from one or two sources and of acetylene from one source, in meteorological and topographical conditions that are adapted to our use of a Gaussian plume model in practice. Concentrations are measured through the methane and acetylene plumes at an appropriate distance from the source, as described below. The known emission of methane is used to validate the inversion results and thus to assess the efficiency of our inversion system. In particular, the fit between these results and the actual emissions is compared with the one obtained with the more traditional computation associated with the tracer release technique to demonstrate, in our experimental conditions, the asset of the statistical inverse modelling framework. In section 2, we detail the theoretical framework of the tracer release technique, the local dispersion modelling, the statistical inversion, and our concept that combines these different techniques. We also give some practical details regarding their application to the monitoring of methane sources, and regarding the use of a Gaussian plume model for relevant meteorological and topographical conditions. Then, we describe the configuration and the results of the experiments conducted in this study to evaluate the potential of our approach (section 3). The results and perspectives of the study are discussed in section 4.

2 Methods

2.1 Instantaneous quantification of pollutant sources using mobile measurements across the atmospheric plumes

The presentation of the atmospheric monitoring techniques below focuses on their specific configuration for the quasi instantaneous estimation of emission rates from gas sources within a targeted site. These techniques apply to gases, that can be considered inert (non reactive) on the short experimental timescales, and thus, the representation of atmospheric transport, linking the emissions to the gas concentrations, can be considered linear. Given that these timescales typically correspond to 1 to 10 hours, it applies to most of the pollutants. In this configuration, several times over the course of a few hours and at an appropriate distance from the site, the concentrations are measured along transect lines

across the plumes of gas emitted by the sources. The emission plumes are associated with an increase of the gas concentrations above the "background" concentration. This background concentration can be characterised by the gas concentrations in the vicinity of the measurement locations that has not been affected by the sources. The increase above the background concentration is proportional to the emission rates (due to the linearity of the atmospheric transport) and it can be identified in the measurements across the plume. Ideally, there should be no other major gas emitter in the vicinity of the targeted site to ensure that, due to the atmospheric diffusion over long distances, the concentrations upwind the site are relatively constant. In such conditions the background concentration can be easily characterised.

The choice of the measurement distances should follow several criteria. The distance has to be high enough such that the transport from the source to the measurement is correctly characterised with a local scale transport model or the proxy from the tracer release, which depends on the spread of the single or multiple targeted sources and thus indirectly on the size of the industrial site, but also on the meteorological conditions like the wind speed and the atmospheric stability. However, the distance should be short enough such that the amplitude of the measured concentrations is high enough compared to the measurement and model precision. This criteria essentially depends on the emission rates due to the linearity of the atmospheric transport from the sources: the larger the source, the larger the signal to measurement, modelling and background noise ratio and thus the higher the precision of the inversions. Finally, the distances should be adapted to the need for conducting measurements on roads located downwind of the site sources (depending on the specific wind directions during the measurement campaigns) when using instruments onboard cars as in this study.

The combination of the estimate of the location and spread of each source and the proxy of the atmospheric transport, which is used to link the gas emission rates from the single or multiple sources of the site to the atmospheric concentrations, is linear. This combination is denoted by the observation operator \mathbf{H} . The relation between the measurement indices of the concentration increase in the emission plumes or "plume indices" hereafter, called the observation vector \mathbf{p} , and the targeted emission rates, called the control vector \mathbf{f} , is given by the observation equation:

$$\mathbf{p} = \mathbf{H}\mathbf{f} + \varepsilon_0 \quad (1)$$

ε_0 represents the sum of errors from the observation operator, in the measurements and in the estimate of the background concentration.

The observation vector is derived from the gas concentrations measured for each cross-section of the gas plume(s). The atmospheric transport proxy can be derived using the relationship between the known tracer emission collocated with the targeted sources and the tracer concentrations in the tracer release technique (section 2.2) or using a local scale atmospheric transport model (section 2.3). Inferring gas emissions from gas concentrations implies inverting the atmospheric transport to express \mathbf{f} as a function of \mathbf{p} . If the size of \mathbf{f} is the same as that of \mathbf{p} , i.e. if the number of plume indices derived from the concentration measurements is set equal to the number of targeted sources, the atmospheric transport matrix \mathbf{H} is a square matrix. If \mathbf{H} is mathematically invertible, i.e., if the problem is not under constrained due to using indices on plumes that overlap too much, and if the measurement, background and observation operator errors ε_0 are ignored, \mathbf{f} can directly be derived from $\mathbf{H}^{-1}\mathbf{p}$ (sections 2.2 and 2.3). If the size of \mathbf{f} and \mathbf{p} differ, or in order to account for the measurement, background and observation operator errors ε_0 , statistical inversion approaches can be performed to retrieve an optimal estimate of \mathbf{f} (sections 2.4 and 2.5).

2.2 The tracer release method

The tracer release method was developed to quantify pollutant emissions and has already been used in a wide range of studies to estimate the sources of various types of gases such as methane (Babilotte et al., 2010), carbon monoxide (Möllmann-Coers et al., 2002) and isoprene (Lamb et al., 1986). This method consists of releasing a tracer gas with a known rate close to the targeted gas source when this source is clearly localized and of measuring both the targeted and tracer concentrations in sections of the downwind emission plumes. When targeting the total emissions of a site with multiple sources, the tracer release is generally located in the middle of these sources, assuming that the site is seen as a point source from the measurement locations.

When both the released tracer and targeted sources are perfectly collocated and constant in time, they have the same spatial and temporal relative variations of their concentrations in the atmosphere, i.e., the plumes of the targeted gas and of the tracer have the same structure ignoring a multiplication factor. In such a configuration, the knowledge of the ratio between the tracer plume index p_t and the tracer controlled emission rate f_t provides a perfect observation operator h , and thus a perfect estimate of the ratio between the targeted gas plume index p_m and the targeted gas emission rate f_m : by ignoring the measurement and background errors, the targeted emission rate can be estimated using the following formula:

$$f_m = f_t \times \frac{p_m}{p_t} \quad (2)$$

Various types of plume indices p can be used (provided that they are consistently derived in the same way for the tracer and targeted gas). The background concentration is generally derived from the measurements before and after crossing the plumes. Then, the plume indices can typically be calculated using the difference between the maximum concentrations (peak heights of the signals) and the background concentration. It can also be derived from the areas between the plume signals and the background concentration (Mønster et al., 2014). When using the tracer release technique, if the sources of the released and targeted gases are perfectly collocated and if their emission rates are constant, both of these approaches provide the same result given that the tracer and targeted emission plumes have the same structure. However, if the collocation of both sources is not perfect or if the targeted emissions vary in time, then the shapes of the emission plumes of the released tracer and of the targeted gas can differ. To minimize the impact of this difference, the ratio of the integrated plumes is generally chosen because this index is less sensitive to the impact of thin turbulent structures than the peak height ratio (Mønster et al., 2014). Other indices have also been tested to overcome this issue like the slope of the ratio between the targeted and released concentrations above the background (Roscioli et al., 2015).

The measurement transects through the emission plumes and the computation from equation 2 are generally repeated several times, typically $n_{tr} = 10-15$ times over an hour window. The mean and standard deviation STD_{tr} of the n_{tr} different results are used as the best estimate and uncertainty assessment for the source quantification. Of note is that strictly speaking, the exact quantification of the uncertainty in the mean estimate should be $STD_{tr}/\sqrt{n_{tr}}$, which will be used here, even though STD_{tr} is often used (Yver Kwok et al., 2015).

Such statistics allow to account, at least partly, for the potential temporal variations of the emissions, for the measurement and background errors, and for the potential impact of the non-perfect collocation of the sources in the selected measurement transects. In order to strengthen the precision of the best estimate, measurement transects with low correlations between the variations of the targeted gas and that of the released tracer concentrations are often ignored in the computation of these statistics. The reason is that such low correlations can be due, for a range of local meteorological conditions, to relatively high background and measurement errors compared to the measured signal, or to a strong difference between the structures of the tracer and targeted gas plumes that prevents to use the tracer plume as an accurate proxy of the local transport from the targeted gas sources to the measurement locations. In the latter case, the difference between the plumes arises from the fact that the tracer emission is not perfectly collocated with the targeted gas emission.

A mislocation of the tracer source too far from the targeted source or its location close to a targeted source whose spread is too large compared to the distance to the measurements can also generate significant biases in the series of computations. Such biases can impact the average estimate of the source without being reflected in the standard deviation of the individual emissions computations nor in the correlation between the tracer and targeted gas concentrations. The impact of the mislocation of the tracer source can be decreased by increasing the distance between the sources and the measurements (Roscioli et al., 2015) but the choice of this distance is often constrained by other considerations as discussed in section 2.1. Approach based on atmospheric transport models have been used to account for the errors from this mislocation (Goetz et al., 2015).

Moreover, the tracer release technique provides an overall estimate of the emissions of a site but, when the site has several sources located quite close to each other, it can hardly be used to provide individual estimates of these sources since even with the use of different tracer release points, the technique in itself hardly provides solutions to separate overlapping tracer or targeted gas plumes associated with different point sources.

2.3 Using local scale transport models

Many types of transport models are used to simulate the dispersion of pollutants at the local scale, i.e. typically over distances from a few metres to 1 or 2 kilometres, from simple Gaussian models to sophisticated CFD (Computational Fluid Dynamics) models that allow to determine turbulent patterns for complex terrain through an explicit representation of reliefs and obstacles (e.g. Baklanov and Nuterman (2009); Hanna et al. (2011)). Beyond the large range of possible model complexity, a common feature of transport model is their ability to represent any potential source geometry.

Therefore, the local scale transport models allow for addressing multiple sources or sources with a significant spread far better than proxies based on collocated tracers. In a configuration similar to that of the tracer release technique where concentration measurements are conducted across the N plumes of N targeted gas sources, the local dispersion models can be used to infer the linear relationship between the emission rates and plume indices in each of the measurement transects. The models are run with a null background concentration unless a strong signal from neighbor sources outside the targeted site need to be accounted for, which is not the case in this study.

In practice, for a given measurement transect, simulations with such models for each individual source (ignoring the other ones), with a unitary emission rate can be used to compute each column of the \mathbf{H} matrix in equation 1. If the plumes of the N sources do not overlap too much and are all discernable in the measurement transect, a relevant selection of N plume indices can be used to dissociate these different sources. In such cases, \mathbf{H} is invertible and the derivation of \mathbf{H}^{-1} from matrix \mathbf{H} is straightforward. Consequently, if ignoring the measurement, background and observation operator errors $\boldsymbol{\varepsilon}_0$, \mathbf{H}^{-1} can be directly used for the inversion of the emission of the N different sources as a function of the N plume indices for each measurement transect:

$$\mathbf{f} = \mathbf{H}^{-1}\mathbf{p} \quad (3)$$

As with the tracer release technique, statistics of the results from the different inversions associated with the different measurement transects can be used to derive a best estimate and its uncertainties. The correlations between the modeled and measured concentrations along the measurement transects can be used to select the most robust inversion cases.

However, the local scale transport models can bear large uncertainties that are ignored by this inversion. These errors can be directly projected into the estimate of the emissions through equation 3, and thus strongly weaken the confidence in the results.

Furthermore, such an inversion can hardly account for the amount of useful information provided by the measurements. Typically, limiting the number of plume indices to the number of targeted sources prevents from analyzing the shape of each emission plume. Such a shape can be an indicator of the measurement, background and observation operator errors $\boldsymbol{\varepsilon}_0$ which can highly impact the inversion results. Finally, with such an inversion, the level of separation between the source plumes has to be evaluated before defining the number of sources that can be inverted separately within a site without solving for an under-constrained problem. When this level of separation is weak, the inversion finds a mathematical solution to equation 3 but this solution can be highly uncertain. The lack of flexibility of such an inversion is thus problematic.

2.4 Statistical inversion

The statistical inversion techniques can address the issues posed by the inversion as described in equation 3 that are discussed above. The Bayesian principle of statistical inversion is to update prior statistical knowledge (i.e. a prior estimate \mathbf{f}^0 and the uncertainties in it) of the emission rates \mathbf{f} with statistical information from observations \mathbf{p} . This update accounts for the statistical uncertainties in the observations (here the measurement and background errors) and in the observation operator \mathbf{H} (Tarantola, 2005). In order to account for several sources within a site, the statistical inversion needs to rely on a local scale transport model to derive the \mathbf{H} matrix.

This theoretical framework allows for a control vector \mathbf{f} and an observation vector \mathbf{p} with different sizes to be taken into account. All sources can thus be “inverted” even if there is not enough information to separate the plumes of some of them. Furthermore, the system can make use of all the information in the measurements to filter the measurement, background and observation operator errors and any signal from the different emissions plumes associated with the different sources.

Assuming that during the measurement campaign the source emission rates are constant, this framework can also be used to assimilate the data from all plume transects to compute the optimal estimation of the emission rates at once. In such a case, the observation vector \mathbf{p} gather plume indices from all the measurement transects and the \mathbf{H} observation operator represents the transport, with various meteorological conditions, from the sources to all the transects. This combination presents advantages over repeating computations for each measurements transect and deriving statistics for the emission estimates out of the ensemble of computations as for the other techniques presented above. In particular, this helps accounting for the fact that the sources of errors do not have the same statistical distribution, e.g., amplitude for each transect. The previous techniques require a selection of the cases when the confidence in the observation operator is good enough to strengthen the robustness of the average. By assigning model and measurement uncertainties as a function of the measurement transect and/or meteorological conditions, the statistical inversion allows the information from each transect to be weighted differently according to its uncertainty when deriving the optimal estimate of the emissions.

The prior estimate of the emission \mathbf{f}^b has to be independent of the atmospheric observations and can be provided by expert knowledge, emission inventories or process-based models. In practice, it is generally assumed that the uncertainties in \mathbf{f}^b , in the observations \mathbf{p} and in the observation operator have unbiased and Gaussian distributions. The prior uncertainty and the sum (henceforth called observation error) of the uncertainties in the observations \mathbf{p} (from the measurement and background errors) and on the observation operator \mathbf{H} are thus characterised by their covariance matrices \mathbf{B} and \mathbf{R} , respectively. Following these assumptions, the "posterior" statistical distribution of the emission rate knowing \mathbf{f}^b and \mathbf{p} is Gaussian and is characterised by its optimal estimate \mathbf{f}^a and its covariance matrix \mathbf{A} given by equations (Bocquet, 2012):

$$\mathbf{f}^a = \mathbf{f}^b + \mathbf{B}\mathbf{H}^T(\mathbf{R} + \mathbf{H}\mathbf{B}\mathbf{H}^T)^{-1}(\mathbf{p} - \mathbf{H}\mathbf{f}^b) \quad (4)$$

$$\mathbf{A} = (\mathbf{B}^{-1} + \mathbf{H}^T\mathbf{R}^{-1}\mathbf{H})^{-1} \quad (5)$$

The matrix \mathbf{A} characterises the unbiased and Gaussian uncertainty in \mathbf{f}^a . If the plume from a source cannot be separated from the other ones, or if the observation errors on the plume indices related to this source are very large, the posterior uncertainty in this source will be large. The \mathbf{A} matrix can thus be used to evaluate the level of constraint on the different sources or on their sum provided by the selection of plume indices, and the robustness of the corresponding emission estimates. One difficulty associated with this method is the need for providing a good estimate of the observation error statistics to the inversion system while it can be difficult to evaluate. Another issue is that even if the system correctly accounts for the transport modelling errors when being well informed about their statistics, the system will derive very uncertain emission estimates if these transport errors are large. The fact that the statistical inversion can warn about this uncertainty through its diagnostic of the \mathbf{A} matrix does not overcome the problem of getting robust estimates of the emissions.

2.5 A statistical inversion based on tracer release and local scale transport modelling

Here, we propose a new concept for the estimation of the gas emission rates combining the tracer release method, local scale transport modelling, and a statistical inversion framework to overcome the issues associated with these different approaches and tools as discussed above. The basis of this new concept is the statistical inversion framework described above assimilating the plume indices from all measurement transects altogether, where the \mathbf{H} matrix is derived from local scale transport model simulations for each point or spread source of a targeted site and each measurement transect.

The main idea is to use the very accurate information on the atmospheric transport in the area of interest from the tracer release method to adjust parameters of the local scale transport models and to assess the statistics of the transport errors. The "optimized" transport model and the statistics of the transport errors are then used for the configuration of the observation operator and of the observation errors in a statistical inversion system. The optimization of the transport model parameters can rely on a range of method, from a simple comparison between ensemble of tracer simulations with different set of parameters and the tracer measurements, to complex tracer data assimilation.

340 The statistics of the misfits between the tracer measurements and the model-based plume indices when using the optimal transport model configuration are used to set up the covariances of the observation (measurement, background and observation operator) errors \mathbf{R} . This requires the conversion of the errors statistics for the tracer gas into statistics of the errors for the targeted gas. Therefore, the statistics of the variability of the measured tracer and targeted gas concentrations are used to normalize the transport errors for the two species as "relative errors", and the assumption is made that the relative transport error are the same for both species. This optimization of the model parameters and/or characterization of the transport errors can be performed for each individual crossing of the plume or for all plume crossings together. If the local meteorological conditions evolve rapidly or if there is a weak confidence in the fact that the parameters to be optimized are the main source of uncertainty in the transport model (such that optimizing these parameters would only compensate for other sources of errors in the transport model), the use of a specific optimization of the model for each plume crossing may be preferable. Using general statistics of the tracer model-data misfits from all plume crossings would prevent weighting the transport error and thus the information for each plume crossing depending on the modelling skills. Deriving different transport errors for each plume crossing requires the extrapolation of the single set of tracer model-data misfits into statistics for each plume crossing. These different options need to be chosen depending on the experimental case.

350 In order to investigate the potential of this approach in a first real test case, we propose a relatively simple first practical implementation of the concept using a Gaussian transport model. CFD models remains sophisticated tools with important computational burdens. The choice of a Gaussian plume model is more relevant for the introduction and first test of our concept but we are aware that it restrains the scope of the real situation that can be investigated.

2.6 Practical implementation for the monitoring of the methane sources using a Gaussian plume model and acetylene as tracer

2.6.1 The Polyphemus Gaussian plume model

365 Gaussian plume models provide a stationary and average view of the pollutant plumes driven by meteorological conditions that are stationary in time and homogeneous in space within the study period and area. This is a decent approximation for the modelling of dispersion over 1–2 minutes (i.e. the typical timescale associated with our experiments) and an area of approximately 1 km² when the wind speed is relatively high. These models cannot precisely account for the local topography and buildings. However, this type of model is suitable for many configurations of industrial sites located in nearly flat suburban to rural areas, and it is easily set up and applied for the simulation of local-scale transport.

In this study, the Gaussian plume model of the Polyphemus air quality modelling system (Mallet et al. (2007) <http://cerea.enpc.fr/polyphemus/>) is used because it has been proven to be adapted for estimating gas emissions from local sites (Korsakissok and Mallet, 2009).

375 Gaussian plume models are based on a simple formula that provides the concentration of the pollutant at a location generated by a point source depending on the weather conditions. The Gaussian plume formula is expressed as:

$$C(x, y, z) = \frac{Y}{2\pi\sigma_y\sigma_z\bar{u}} \exp\left(-\frac{(y-y_s)^2}{2\sigma_y^2}\right) \times \left[\exp\left(-\frac{(z-z_s)^2}{2\sigma_z^2}\right) + \exp\left(-\frac{(z+z_s)^2}{2\sigma_z^2}\right) \right] \quad (6)$$

where C is the concentration of the pollutant at a location of coordinates (x,y,z) , Y is the source emission rate, and \bar{u} is the wind speed. In this formula, the x axis corresponds to the wind direction, y_s is the pollutant source ordinate and z_s is the release height above the ground. As both studied gases are poorly soluble and chemically inert for the considered dispersion time scale, it is relevant to neglect the mass loss due to dry deposition and assume a total reflection from the ground. σ_y and σ_z are the horizontal and vertical Gaussian plume standard deviations and characterise the atmospheric conditions during the measurements. The modelled concentrations are strongly dependent on these two parameters. Polyphemus proposed several ways to parameterize these constants: the Doury formulas (Doury, 1976), the Pasquill-Turner formulas (Pasquill, 1961) and the Briggs formulas (Briggs, 1973).

Briggs parameterization is the most adjustable parameterization of Polyphemus: not only does this parameterization consider the stability of the atmosphere via six classes from A (extremely unstable) to F (extremely stable) by taking into account wind speed and solar irradiance but also the type of environment where the emissions occurred with an urban mode when the site is surrounded by buildings and a rural mode for the isolated sites (by changing the roughness factors). The standard deviations with Briggs parameterization are given by the following equations:

$$\sigma_y = \frac{\alpha x}{\sqrt{1 + \beta x}} \quad \text{and} \quad \sigma_z = \alpha x(1 + \beta x)^\gamma \quad (7)$$

where x is the downwind distance from the source and α , β and γ are coefficients that are dependent on the stability classes. All these coefficients can be found in Arya (1999).

Different source spatial extensions can also be created in this model. However, its configuration imposes the emission f_i of a given source to be spread homogeneously over its extension. The Gaussian plume model cannot represent the dispersion pattern due to turbulent structures at fine spatial and temporal scales. However, it is expected that the statistical inverse modelling framework exploiting all measurement transects altogether allows for filtering the average plumes from the targeted sources. Therefore, it is expected that if using a high number of measurement transects, the Gaussian plume model should be relevant for catching such an average plume and that the transient turbulent patterns in the measurements would generate a sort of noise on the emission estimates without biasing it.

2.6.2 Adjustment of the stability class underlying the Briggs parameters and estimate of the Gaussian model errors using the tracer data

The application of the new statistical inversion strategy described in section 2.5 with the Polyphemus Gaussian transport model we propose relies on the optimization of the stability class underlying the Briggs parameters and of the plume direction as a function of the tracer measurement transects. In practice, we conduct wind measurements in our experiences. In such cases, the correction of the Gaussian plume direction should not be needed, but the section 3.2 will describe practical issues which require such a correction of the model plume direction.

For each measurement transect, the method consists in running different model tracer simulations with different stability classes. They are all forced with the known tracer emission rate. The model plume direction is adjusted so that the measured plume and simulated plumes are aligned. The stability class whose corresponding simulation of the tracer concentrations best fits the tracer concentration measurements is taken as the optimal one. The fit is quantitatively checked for the plume indices chosen for the definition of \mathbf{p} , but it is also checked in a qualitative way by analyzing the shape of the modelled and measured signals. The estimate of the Gaussian model errors is based on statistics of the misfits between the modeled and measured tracer plumes indices.

2.6.3 Monitoring of the methane sources using acetylene controlled release

This method is tested for the quantification of methane sources using acetylene as a tracer gas. Both of these gases are inert and can be considered non-reactive at the time scale and over the space scales corresponding to the time and distance between the release of molecules at the source and the measurement of concentrations downwind in the plume, with the lifetimes of methane and acetylene being approximately 10 years and 2–4 weeks, respectively (Logan et al., 1981). In this study, the methane and acetylene concentrations are measured in a continuous manner along a line crossing the emission plumes using an accurate analyser placed in a car. Our preliminary analysis shows that we obtain satisfying results when concentrations are typically measured at a distance of 100 to 1000 metres from methane sources of 1500 to 100000 $\text{gCH}_4 \cdot \text{h}^{-1}$ and spread within an area of $100 \times 100 \text{ m}^2$ to $500 \times 500 \text{ m}^2$.

3 Evaluation of the concept with controlled release experiments

3.1 General principle of the controlled experiments

The following sections describe the experiments under controlled conditions for both acetylene and methane used to evaluate the statistical inversion framework detailed in section 2.6 and more generally

to give insights on the potential of the approach proposed in this study and presented in section 2.5. A campaign was organized during two days of March 2016 at the Laboratoire des Sciences du Climat et de l'Environnement (LSCE) in France (longitude: 48.708831°, latitude: 2.147613°, altitude asl: 163 m). The experimental conditions were selected to be favorable to the use of a Gaussian plume model to simulate the atmospheric transport. One or two methane sources and one acetylene point release were generated with cylinders in the parking lot of the LSCE, which is located in a rural area in the southern region of Paris. The topography of this area is very flat, and only few buildings of small size can influence the atmospheric transport from the parking lot to the road where the concentrations are measured. This road is located approximately 150 metres away from the controlled sources. No major methane or acetylene sources in the vicinity of the LSCE could disturb the measurements. Each measurement day was selected by taking the weather forecast into account and choosing days with a strong enough wind coming from the north to be able to measure the emissions from the parking lot on the measurement road. The average weather conditions of each campaign are summarized in table 1.

During this campaign, the methane and acetylene sources were dispersed in four different configurations to estimate the accuracy of the proposed method and the uncertainties depending on whether the tracer gas is perfectly collocated with the methane source or not. For each configuration, the methane and acetylene emission plumes were crossed 20–40 times (see table 1), and each series of crossings were performed on the same day on a timescale of 1-2 hours. The observed increases in the acetylene and methane concentrations within the plumes ranged between 3–15 ppb and 50–500 ppb, respectively. Configurations 1, 2 and 4 were tested in the afternoons between 13:30 to 16:30 UTC while configuration 3 was tested in the morning between 10:00 and 12:00 UTC (see Figure 1).

The following sections describe the different components of the experimental and modelling systems used for the inversion of the methane sources and the results from both the tracer release technique and the combined statistical approach. These results are compared with the known methane emission rate to illustrate the ability of each method to derive a good estimate of the emissions. Statistics of uncertainties are also derived for the two methods based on the statistical frameworks described in section 2 but also based on Observing System Simulation Experiments (OSSEs) with pseudo-data.

Of note is that for the sake of clarity and simplicity, we avoid analyzing the results that would be obtained with a modeling framework where the observation operator is truly inverted (see section 2.3). Such results would not have supported the analysis of the potential of the combined approach compared to the traditional tracer release technique, and discussing whether, in this approach, the Gaussian modeling configuration should be influenced or not by the parameter optimization based on the tracer data would be uselessly complicated.

3.2 Analytical equipment

Downwind gas concentrations were measured using a G2203 cavity ring-down spectrometer (Picarro, Inc., Santa Clara CA), which continuously measures acetylene (C_2H_2), methane (CH_4) and water vapor (H_2O). Based on infrared spectroscopy, the high precision of the system (precisions of 3 ppb and < 600 ppt for methane and acetylene, respectively, on 2 second interval) is due to its very long path length ($\simeq 20$ km) and the small size of its measurement cell (< 35 mL). Mobile measurements with such an instrument have already been successfully performed and published in previous studies (Mønster et al., 2014; Yver Kwok et al., 2015), thus demonstrating the potential of this method. The measurement error encompasses the precision given here but also the fact that the acetylene and methane are not measured at the exact same time and frequency. Indeed, acetylene is measured every second while methane is measured every other second. At the scale of our measurement (less than a minute to cross a plume), this can impact the error significantly.

Before the experiment, the instrument has been tested in the laboratory. It showed a good linearity over a large range of mixing ratios and a good stability over time with small dependency to pressure and temperature. To control for a drift, we measured a gas with a known mixing ratio (calibrated with a multi-point calibration in the laboratory) before each series of measurements in order to ensure the good analytical performances of our instrument. Moreover, in the tracer released method and the combined approach presented in this study, we are interested in the increase of concentrations due to the tracer and targeted point sources above the background signal (i.e. the plume indices) more than in the absolute value of the measurements. Thus, an offset of the measured concentrations will not impact our estimates.

During the field campaigns that we organized for this study, wind speed and direction were taken

from the meteorological station installed on the roof of the nearby laboratory at about 7 m high. The mobile system was set up in a car and powered by the car's battery. The air sampler was placed on the roof at approximately 2 metres above the ground with a GPS (Hemisphere A21 Antenna) to provide the location of the measurements. The sampled air was sent into the instrument by an external pump system allowing a short inlet lag between the sample inlet and the measurements (less than 30 seconds). Despite the relatively fast response time of this system, this more or less constant inlet lag introduced a spatial offset when comparing the measured and modelled tracer or methane concentrations. This spatial offset is the same for methane and acetylene and is well characterised by the comparison between the modelled and measured acetylene plumes. In our combined statistical approach, it is thus well accounted for when comparing the modelled and simulated methane plumes thanks to the correction of the Gaussian plume direction according to the acetylene data. Therefore, this correction is ignored hereafter. Of note is that this offset should not impact the computation of a single methane plume index such as the maximum of a single emission plume or its area above the background concentration. Therefore, such an offset has no impact on the tracer release technique. However, when targeting the quantification of several methane sources with overlapping plumes using the statistical inversion, the need for separating these different plumes requires a good correction of such an offset.

3.3 Tracer and target gas release

Acetylene is commonly used as a tracer. Due to its low concentration in the atmosphere ($\approx 0.1\text{--}0.3$ ppb), any release is easily detected. Acetylene also presents the benefit of being inert, and thus, negligible loss during the transport process is expected (Whitby and Altwicker, 1977). Other gases are suitable as tracers, such as SF_6 , but acetylene is preferred because it is not a greenhouse gas. However, due to its flammability, its use requires specific precautions.

An acetylene cylinder (20 L) containing acetylene with a purity $> 99.6\%$ was used as the tracer source. A methane cylinder (50 L) with a purity of 99.5% was used for controlled methane release. The flows of both gases were controlled by a 150 mm flowmeter (Sho-rate, Brooks) able to measure fluxes between 0 and $1500 \text{ L}\cdot\text{min}^{-1}$. The different acetylene and methane emission rates were checked by weighing the cylinders before and after each test and timing the release duration. The flow rate calculated with the mass difference was systematically in good agreement with the flow rate read on the flowmeter. Therefore we believe that there was no important variability of the acetylene and methane release during our experiments. The amount of acetylene emitted was adjusted such that its emission plume can be detected on the roads where the measurements were performed while keeping it at the lowest rate possible to limit the risks associated with its flammability. In this study, we used emission rates from 65 to $90 \text{ g}\cdot\text{h}^{-1}$ for acetylene. During the measurement campaigns, the cylinders were attached with straps to a fixed frame to avoid any accidents.

3.4 Tested configurations of the gas releases

This section details the four configurations used during this campaign for estimating the accuracy of the proposed concept and the uncertainties linked to the misplacement of the tracer gas regarding the methane source (figure 2). The first configuration consisted of a collocated emission of acetylene and methane. This configuration enabled us to estimate the accuracy of the method and our system under optimal conditions. One cylinder of methane and one cylinder of acetylene were placed on the parking lot and connected together by a tube with a length of a few metres. This system aimed at ensuring the mixing of both gases and was designed to be as close as possible to the ideal situation in which methane and acetylene are emitted at the same location and under the same conditions. In principle, under such conditions, the tracer concentration to emission ratio should provide a perfect proxy of the methane transport and the tracer release technique should provide better estimates than the statistical inversion that relies on an imperfect, although optimized, modelling of the methane plume. Still, both techniques should be hampered by measurement and background errors.

In reality, in industrial sites, methane source locations are not always well known, or it may be difficult to access these sources and place a tracer cylinder next to them. The second and third configurations tested the impact of non-collocated emissions of tracer and methane. To represent this situation, one cylinder of methane and one cylinder of acetylene were used, and the methane cylinder was moved i) approximately 60 metres downwind from the acetylene bottle location (second configuration) and ii)

540 approximately 35 metres laterally compared with the wind direction (third configuration). Of note is that during these two experiments, the wind was blowing from the North, i.e. it was perpendicular to the measurement transects along the road, south of the sources.

545 Finally, within real industrial sites, several sources of methane may be encountered. The fourth configuration tested the influence of having several methane sources on the estimation of their fluxes when one tracer source is used. With this configuration, we also evaluate the ability of the combined statistical approach to estimate the emissions for each individual methane source. For this purpose, a system of two tubes was connected to the methane cylinder, splitting its exhaust into two locations approximately 35 metres apart. Of note is that during this experiment, the wind was blowing from the North-East, i.e. it was not perpendicular to the measurement transects along the road. The acetylene cylinder was collocated with one of the exhausts.

550 The advantage of the combined method proposed in this study over the traditional tracer release technique (which relies on the collocation of the target and the tracer gas sources) to infer the total emissions from a site should be revealed in the second and fourth experimental configurations. In theory, and in homogeneous meteorological conditions, due to the linearity of the atmospheric transport of methane, and when the wind direction is perpendicular to the measurement transects, the shift of the methane sources in a direction perpendicular to the wind speed and parallel to the measurement transects should just shift the emission plumes along the measurement transects. It should not impact the plume indices from the measurement transects and thus the results from the tracer release technique. Therefore, in idealistic conditions, in the third experimental configuration, the tracer release technique should still provide better estimates than the combined approach. However, in practice, during experiments with the third emission configuration, neither the shift between the cylinders nor the measurement transects (along the slightly curvilinear road) were perfectly perpendicular to the wind direction, and they were not perfectly parallel between them. Therefore, the combined approach has potential to yield better emission estimates than the tracer release technique with the third configuration as well. Finally, it can provide estimate for both sources in the fourth configuration, while this cannot be achieved with the tracer release technique in our experimental framework due to the strong overlapping of the plumes from the individual sources (see section 3.8).

565 The time series of acetylene and methane measurements for each tracer release experiment are shown in figure 1.

3.5 Definition of the background concentration and of the plume indices

570 In this study, two different definitions of the plume indices to build the observation vector \mathbf{p} are used but they are both based on the integral of areas between the concentrations within the plumes and the background concentration.

575 The portions of plume concentrations and of background concentrations in the measurement transects are defined "by eye". The portions of background concentration used for the computations are restricted to $\simeq 5$ s before and after the portions of plume concentrations. In many cases, the increase of the concentrations due to the plumes is clear and the portions of plume and background concentration easy to define. However, in other cases the background variations near the plumes and the turbulent patterns at the edge of the plumes can have comparable amplitude so that the definition of these portions is more difficult (Figure 1). For each plume, the background concentration value used to compute the plume index is taken as the average concentration over the background portions of the transect.

580 When we investigate the tracer data or when we estimate the emission rate of a single source of methane, i.e. in configurations 1, 2 and 3, and in configuration 4 for the tracer release technique only, the plume indices are defined as the integration of the entire plume concentrations above the background. In this case, the observation scalar p (when applying the tracer release technique to each transect) or vector \mathbf{p} when conducting the combined statistical inversion by gathering data from all transect into a single vector, are denoted p^{ent} and \mathbf{p}^{ent} respectively.

590 When we estimate the emission rates of the two sources of methane with the combined approach in configuration 4, the portion of observed methane and acetylene increase within the plumes is divided into five slices of equal time (and identical for the methane and the acetylene). For each slice of a given transect, an index p_{slc} is defined as the integration of the concentrations above the background in this slice. The observation vector \mathbf{p}^{slc} gathers all these indices.

3.6 Optimization of the Gaussian plume model parameters

In the Polyphemus Gaussian plume model, the definition of the plume indices is consistent with the one in the measurements, and in particular it follows the same definition of the plume portions or slices along the measurement transects.

For each measurement transect, the optimization of the Briggs stability class of this model is based on the fit to the acetylene plume index only. Since we do not have access to the solar irradiance, comparing the selected stability class to the theoretical one is impossible. According to the table of Pasquill, there are three stability classes that correspond to the 2 to 4 m.s⁻¹ measured wind speed during our experiments: the classes A and B and C. However, for a given wind speed, there is only two choices, A and B, or B and C. We have verified that the selected stability class is systematically consistent with these two theoretical options. Choosing one over the other can modify the simulated plume indices by a factor 2 to 3.

We also checked for each measurement transect that the model error is not too large. In some cases, the model cannot "reasonably" reproduce the observations due to the presence of large turbulent structures or due to transport conditions that are extremely unfavorable for the model (due to swift wind change or low wind conditions). In such situations, there is no Briggs stability class that allows for the model to fit approximately the acetylene plume index. Finally, we decided to remove transects from the analysis when the relative error between the modelled and measured acetylene plume indices was higher than 70%. This value of 70% is an empirical choice but it corresponds to very large modelling errors and all cases kept for the analysis had relative uncertainties well below this 70% threshold. In theory, the strategy of computing the statistics of the model error as a function of such misfits should ensure that the weight given to these transects in the inversion is low. However, in practice, we conservatively prefer to remove transects for which the confidence in the model is extremely low. This evaluation leads us to ignore 30% of measurement transects when applying the combined statistical approach.

Figure 3 illustrates the results of the model parameterization selection. In this example, which corresponds to the 5th transect of the measurements for the configuration 2 when the wind speed was 2.9 m.s⁻¹, the tracer concentrations modelled with the stability class B best fit the measured concentrations, which are represented in black.

3.7 Estimation of the biases of the tracer release method due to the mislocation of the tracer with theoretical model experiments

When using the tracer release technique, defining the optimal estimate of the emissions from the n_{tr} selected transects as the average estimate from the application of equation 2, and using $STD_{tr}/\sqrt{n_{tr}}$ as an estimate of the uncertainty in this optimal estimate of the emissions, fully ignores any potential bias in the method. However, in our experiments, the mislocation of the tracer emission has a strong potential to generate a bias in the computations in addition to random errors (that are caught by the variations of the results between the different measurements transects) since the measurements are taken in a relatively narrow range of positions south of the sources. Such a problem applies to many of the tracer release experiments where the measurement are always taken from the same area (e.g., due to the need for using roads).

Here, we use OSSEs (Rayner et al., 1996; Chevallier et al., 2007) with the Gaussian plume model whose stability class is optimized with the tracer data to estimate the bias that can arise from the spatial offsets between the tracer and methane sources. The bias estimates will be used to complement the assessment of uncertainty in the results from the tracer technique, except in the first configuration of the experiments, for which there is no offset between the methane and acetylene sources. As discussed in section 3.4, the "lateral" (i.e. orthogonal to the wind direction and parallel to the road) offsets between the methane and tracer sources in the third experimental configurations should have a weak impact on the tracer release computations. There should be far larger bias associated with the downwind shift of the unique methane source in the second experimental configuration and to the complex shift of one of the methane source when the wind was not blowing perpendicular to the measurement transects in the fourth experimental configuration.

In the OSSEs, we assume that the true methane and acetylene emission rates are those used for the experiments with real data. The synthetic methane and acetylene concentrations are simulated with the Gaussian plume model forced with these emission rates and similar weather conditions as during

645 the campaign. The corresponding emission plume transects for both gases are extracted along the same
paths as during the campaign. Finally, equation 2 is applied with the acetylene and methane plume
indices from these simulations and the acetylene emission rate, and the resulting methane emission rate
is compared with the actual one. The comparison provides a direct estimate of the bias associated with
650 the spatial offset between the acetylene and methane sources since in these computations, stationary
conditions are implicitly assumed, since the same model configuration is used to simulate the acetylene
and methane concentrations (rejecting any error that could be related to the atmospheric transport
itself), and since we ignore the background and measurement errors.

In the following, we characterise the biases by their absolute value and the fraction of the actual
source that they represent. The bias is estimated to be 69% for configuration 2, 12% for configuration 3
655 and 56% for configuration 4. Considering the amplitude of these errors, we can expect that our combined
statistical approach has a high potential for providing better estimates than the tracer release approach
for configurations 2, 3 and 4.

In order to get a better characterization of the biases as a function of the upwind or downwind shifts
of the tracer source compared to the targeted source and as a function of the distance between the sources
660 and the measurement locations, we conduct further OSSEs for theoretical experimental configurations
with one methane and one acetylene source only, and using northern wind conditions as was measured
during the first experimental configuration.

Upwind and downwind offsets from 20 to 200 metres between the methane and tracer sources are
tested with OSSEs, with hypothetical measurement transects perfectly orthogonal to the plumes (wind)
665 directions at different distances from 100 to 2750 metres from the methane source.

The corresponding estimates of biases are presented in figure 4, with the results for the downwind
and upwind shifts of the acetylene source provided in figures 3a and 3b, respectively

When the tracer is released upwind of the methane source, the emission rate is overestimated because
of the vertical atmospheric diffusion, which makes the integral of the released tracer concentrations
670 through the measurement of emission plume near the ground lower than if both sources were collocated.
The opposite occurs if the released tracer is placed downwind of the methane emission location.

When the tracer source is either upwind or downwind of the methane source by more than 100
metres and the measurements are taken at less than 300 metres, the bias exceeds 40%. The biases due
to upwind shifts are generally similar to the biases due to downwind shifts over the same distances. When
675 the measurement distance increases, the impact of the shift between the sources decreases. When the
measurements are taken at more than 1200 metres, the bias becomes less than 20% but at such distances,
with the emission rates used in our experiments, the signal to measurement and background noise ratio
would likely be too small, using these instruments, to derive precise estimates of the emissions.

3.8 Tracer release method estimates

680 Figure 5 presents one example of the measured acetylene and methane cross-sections used for calculating
the methane emission rate for each campaign. For the first campaign, both the acetylene and methane
profiles are similar due to the collocation and the mixing of the sources, but we can still observe a
significant difference between both emission plumes due to measurement and background errors. The
shift between the sources is reflected by a smaller relative amplitude and a higher relative width of
685 the acetylene plume compared to the methane plume in configuration 2 than in configuration 1 and
by a lateral shift of the acetylene plume compared to the methane plume in configuration 3. The two
overlapping methane emission plumes, one superimposed with the acetylene plume, can be distinguished
on the example given for the fourth configuration.

In this section, the uncertainties in the optimal (i.e., average) estimates of the sources are characterised
690 by the random uncertainty which is given by the variations of the results between the measurement
transects, $STD_{tr}/\sqrt{n_{tr}}$, by the bias due to the mislocation of the tracer (see section 3.7 above), and by
the standard deviation of the total uncertainty being taken as the root sum square of these two terms.
Table 2 lists the estimated methane emission rates and the methane emission rates actually released for
each tested configuration.

695 These results confirm that the closest estimates to the actual methane rates are obtained for the first
and the third emission configurations with a relative difference of 14% and 11% respectively. However,
they are surprisingly slightly higher for the first configuration than for the third one. Furthermore, these
errors are relatively high for the tracer release technique. They are mainly due to the variations in

the background concentrations for methane, but also in some cases for acetylene. For example, the methane background can range between 2079 and 2099 ppb from one crossing to another for the first configuration or between 2012 and 2031 ppb between transects for the third configuration. Moreover, the standard deviations of the methane concentration within the background portions used to compute the background concentration can reach 9 ppb and 1 ppb for the acetylene. These variations characterise the level of uncertainty in the background concentration and they are significant compared to the amplitude of the plumes. The measurement errors associated with the lagtime between the methane and tracer concentrations may also play a significant role in the level of error associated to the estimates from the tracer release technique. However, the instrumental precision should not be responsible for such an error in the emission estimated since its amplitude is much smaller than the typical signals measured throughout the experiments (figure 1 and 5). The relative differences between the actual rates and the tracer release estimates are much more important for the second and the fourth configuration, 32% and 67% respectively. The comparison between these results and those estimated in the first and third configuration indicates that in the latter cases, the observation operator errors associated with the mislocation of the tracer are much more important than the impact of the measurement and background errors. These error estimations based on direct comparison of the known emission rates are relatively well reflected by the uncertainty estimates, which are much lower for configurations 1 and 3 than for the second and fourth one, both in terms of random error and in terms of biases.

3.9 Combined approach

3.9.1 Configuration of the statistical inversion parameters

In this section, we provide details on our definition of the prior estimate of the sources \mathbf{f}^b , of the covariance matrix of its uncertainties \mathbf{B} , and of the covariance matrix of the observation errors \mathbf{R} that are needed for the application of equation 4 underlying the statistical inversion.

Here, we assume that the measurement and background errors are negligible compared to the transport errors, and thus that the observation errors can be summarized to the transport errors. This assumption arose from the relatively high values taken by the transport error estimates. The modelled vs. measured tracer plumes indices, and their product by the ratio between the methane and tracer measured plume indices are thus used to set up the variances of the observation error in the inversion configuration, i.e., the diagonal of the covariance matrix \mathbf{R} . In the case of a unique methane source, for each measurement transect, we use the absolute value of the difference between the modelled vs. measured plume indices to set up the standard deviation of the observation error for the corresponding observation. When there are several methane sources within a site, for each slice of the measurement transects (see section 3.5), we use the absolute value of the difference between the modelled vs. measured plume indices to set up the standard deviation of the observation error for the corresponding observation. We assign a minimum value for these standard deviations to prevent one transect or slice of a transect to dominate too much over the others in the inversion process. In the least squares minimization process associated with the statistical inversion, a data assimilated with a considerably lower observation error than the others may fully drive the inversion results. However, for some transects, an excellent fit may occur between the model and the measurements in terms of plume indices (i.e., integration of the emission plume concentrations over the background) whereas the shapes of the modelled and measured tracer plumes can be significantly different, revealing some significant observation errors. Applying a threshold to the observation errors limits the impact of their underestimation through the objective comparison between the modelled and measured plume indices. We make the assumption that there is no correlation of the transport errors, and thus of the observation error (assuming that it is dominated by the transport errors) from one slice to the other slice of a given transect or from one transect to another one such that the \mathbf{R} matrix is set up diagonally.

The typical prior knowledge \mathbf{f}^b on the emission rate, from waste treatment sites, farms, or gas extraction or compression sites from process models, typical national- to regional-scale factors is generally highly uncertain. It can bear more than 100% uncertainty and for many of these sites, the order of magnitude of the uncertainty in the emissions is not known. Despite working in the framework of a controlled release experiment, we attempt to set up the inversion system to have the same conditions as when monitoring the emissions from such sites. We thus set up the prior estimate of the methane emission rates to 1800 g.h^{-1} and the standard deviation of the prior uncertainty in these rates to 80%

of this prior value. This ensures that the prior knowledge in these experiments was poorly known by the system, and that it had a weak impact on the results. In general, there is no correlation between the prior uncertainties in the methane emissions from different targeted sources within a site since they generally correspond to different processes (e.g. the aeration process and the clarification process in wastewater treatment plants (Yver Kwok et al., 2015)). Therefore, here, the \mathbf{B} matrix is set up diagonally.

3.9.2 Results

Figure 6 presents examples of results obtained using the combined statistical approach with one or several methane sources. The behaviour of the inversion system and the values in the concentration and observation space are illustrated for one transect only (for the 3rd transect of the first configuration and for the 38th transect of the fourth configuration). It shows that the posterior estimates of the emissions have a much better fit of the simulated concentrations and plume indices than the prior emissions.

Table 2 presents the methane emission rates estimated with the combined approach for each tested configuration. We also analyse the covariance matrix \mathbf{A} of the theoretical uncertainty in the emission estimates when using the statistical approach (equation 5), which provides a complementary assessment of the reliability of the results and of the level of separability between the two methane sources when using several of them in the experiments.

For the first and the third configurations, the statistical inversion gives relatively good estimates of the methane emission rates as the tracer release method, with relative differences between the actual rates and the combined approach estimates of 15% and 7% respectively. As expected, the tracer release technique provides better results for the first configuration. However the corresponding difference or relative error is very small and the combined statistical approach provides better results in the third configuration.

Furthermore, the combined approach derives relatively good estimates for the second and the fourth configurations as well, contrary to the tracer release method. Indeed, for both of these experiments, the relative differences between the actual rates and the combined approach estimates are 16% and 4% respectively. Since being impacted by the background and measurement errors as well as the tracer release technique, this approach still provides relative errors that exceed 15% for configurations 1 and 2 but they get lower than 10% for the third and fourth configuration.

In all cases, the statistical inversion predicts a very low standard deviation of the posterior uncertainty in the emission estimates for each configuration. For the fourth configuration with two methane sources, the approach fails at deriving precise estimates of each source due to the important overlapping of their emission plumes during most of the crossings. Indeed the system attributes almost all the emissions to one of the two sources and none to the other one. The diagnostic (through the computation of \mathbf{A}) of negative correlation (-0.41) of the posterior uncertainties in these two sources supports the assumption that there is a weak ability to separate the signal from each source due to their overlapping, and that it is the main source of error in their individual estimates.

4 Discussions

We propose a new atmospheric concentration measurement-based concept for instantaneous estimates of gas emissions from point sources or more generally from industrial sites. This concept is based on a combination of the tracer release technique, local scale transport modelling and a statistical inversion framework. The idea is to optimize the model parameters based on the knowledge provided by the tracer release and concentration measurement and to exploit tracer model – measurement misfits to prescribe the statistics of the modelling error in the statistical inversion framework. Compared to the traditional tracer release technique, the method has the advantage of exploiting the knowledge on the atmospheric transport provided by the known tracer release and measured concentration without relying on the collocation of the tracer emission and of the targeted gas emission, which is not always easy in real cases. The statistical framework can account for the different sources of uncertainties in the source estimate, can solve different targeted sources together and can consider any valuable number of pieces of information in the measurement of the targeted gas for such an inversion.

The general results from our experiments indicate that both the tracer release technique and the combined statistical inversion system can provide good instant estimates of the total methane emission

rates for each of the four source configurations. However, the results when using the most favorable configurations of controlled emission where the methane source(s) are collocated (configuration 1) or nearly aligned with the tracer source in the direction of the measurement transects that is nearly orthogonal to the wind direction (configurations 3) can still bear more than 10% relative errors. This is relatively high for the tracer release technique compared to what has been obtained, e.g., by Allen et al. (2013). Furthermore, for both the tracer release technique and the combined statistical inversion, the best results are not obtained for the most favorable controlled emission configuration when the acetylene and methane sources are collocated, and thus when the acetylene should provide a very precise (perfect if ignoring the measurement and background uncertainties) proxy of the methane atmospheric transport. The results in the other configurations should be hampered by larger uncertainties in the representation of the atmospheric transport from the methane sources to the measurement locations due to the local variations of the wind from the methane to the acetylene sources.

Actually, the variations of the transport conditions from one experimental configuration to the next reveal to be the strongest driver of the precision of the results in our study. It changes the turbulent patterns and thus the transport errors when using the model or when using the tracer with a mislocated source. It also changes the typical amplitude of the tracer and methane signals, and thus the signal to measurement and background noise ratio. The signal to measurement and background noise ratio is critical and strongly influences the inversion precisions since for many measurement transects, our measurement and background errors appear to be significant compared to the amplitude of the measurements. The pure acetylene or methane measurement errors themselves seem to be negligible given the typical concentrations measured in this study. However, the small timelags between the acetylene and methane measurements are presumed to raise significant uncertainties in the comparison between acetylene and methane data. The variations in the background concentrations for methane, but also in some cases for acetylene, also prove to be high enough to raise uncertainties in the single "background value" that should be used for the computation of the so-called plume indices, i.e. the integral of the increase of the concentrations above the background within the plumes. In any cases, the weight of the measurement and background uncertainties partly arise due to the relatively small sources of methane investigated in this study. Due to the linearity of the atmospheric transport, we can anticipate that the results would have been better if the methane emission rates would have been larger due to the increase of the signal to measurement and background noise ratio. In real application cases, the methane industrial emissions are definitely higher than the controlled emissions used in our experiments and we can thus expect the issue of the measurement and background errors to be less critical. Furthermore, we ignored these errors when deriving the covariance of the observation errors in the statistical inversions while several indicators could have been used to characterise their statistics. We could thus help the combined statistical inversion system better account for them when they are significant.

Despite these issues, this set of experiments clearly confirmed our expectations regarding the tracer release technique and the combined statistical inversion. In the configuration with the methane and acetylene sources collocated, the tracer release method provides better results than the statistical inversion since the latter is impacted by significant transport errors in addition to background and measurement errors while the tracer release technique is impacted by the last two sources of errors only. The optimization of the Gaussian plume model using the acetylene data still proves to be efficient to limit the transport errors and the accuracy of the statistical inversion is still close to that of the tracer release technique for the first experimental configuration.

In the other experimental configurations, which are representative of frequent situations in industrial sites when the tracer cannot be released close to the single or multiple targeted sources, the combined statistical inversion provides better results than the tracer release technique. Our OSSE demonstrates that the mislocation of the released tracer can induce large errors when considering moderate distances between the tracer and the targeted sources even with much larger distances between the measurements and the sources. In these cases, our experiments with real data illustrated that the calibration of a Gaussian plume model using the tracer release method and the integration of the calibrated model in a statistical inversion framework help to reduce this error. The better behavior of the statistical inversion compared to the tracer release technique cannot be explained by a stricter selection of the measurement transects by the former: we recomputed the results from the tracer release technique when limiting the selection of the transects to that of the combined statistical approach and found very similar results (33% of error instead of 32% for the second configuration). On the opposite, the need for using a stricter selection of measurement transects that fit with the Gaussian plume model can be seen as a weakness

of the combined inversion approach. The reduction of the transport error when using the model rather than the tracer with a mislocated source is the best explanation for the improvement of the results with the statistical inversion.

However, our results from the experiment with the fourth configuration of the controlled emissions fails to demonstrate the skills of the atmospheric inversion for providing precise estimates of the different emission rates from the multiple sources within our site. At least, it shows that the statistical inversion could diagnose by itself, with the estimate of the posterior uncertainty covariance matrix, indications that the two targeted sources of methane were too close such that their plumes were hardly separated by the inversion in this fourth configuration.

The much lower uncertainties associated with the statistical inversion results seem to confirm that they are more robust than those from the tracer release method. However, even though the uncertainty estimates in both methods are supposed to cover all sources of uncertainties, they rely on very different assumptions regarding these sources of uncertainties and on very different theoretical derivations. In particular the statistical inversion ignores biases while we explicitly accounted for biases in the tracer release technique. Furthermore, unlike the estimate of uncertainties for the tracer release technique, the statistical inversion ignores the variations of the methane observation values and methane model data misfits from one transects to the other one. It strongly relies on our characterization of the transport errors and prior uncertainties. We tried to rely on an objective quantification of the transport errors and we used such a high uncertainty in the prior flux estimates that this estimate did not weight in the statistical inversion. However, the derivation of the transport error still relied on strong assumptions regarding its structure, and in particular regarding its spatio-temporal correlations. All of this makes the comparison of the error bars for the two methods difficult and weakens the reliability on the quantification of the uncertainties in the results from the statistical inversions, especially since they appear to be very low for all experiments. These uncertainties should be used cautiously as an indicator of the relative behavior of the system rather than an absolute indicator of the result precision.

These results with a rather simple implementation of the combined statistical approach using a Gaussian plume model are highly promising for our concept, and they demonstrate its potential for providing better results than the traditional tracer release technique. However, the results from this study should not be generalised into a comprehensive evaluation of the robustness of the concept. Here, the practical use of a Gaussian plume model is made relevant by the choice of the experimental conditions over a flat terrain and for relatively stationary and homogeneous wind conditions. Such conditions may be difficult to gather when conducting real measurement campaigns for industrial sites. This new method cannot be generalised if relying on a Gaussian plume model, while the tracer release technique is adapted to a far larger range of meteorological and topographical conditions. There is a need of studies to investigate the use of more complex types of local transport models (e.g. Lagrangian models driven by diagnostic wind flow model or 3D flow fields from CFD simulation) to apply the combined statistical approach to such a range of conditions.

Furthermore, as indicated above, the turbulent patterns induced significant transport errors that participated to the significant uncertainties in the inversion results. The strict selection of the measurement transects that can be exploited by the inversion system is strongly related to the poor ability of the Gaussian plume model to simulate many of them. This is demanding in terms of measurements, many transects being needed to ensure that a significant set will be used for the statistical inversion. At last, for the optimization of the Gaussian plume model settings, the variable selection of stability classes representative of less than 15 minutes measurement transects is questioning. Even though in the method, the fit of the model to the tracer data is the only critical criteria (the consistency between the stability class and the meteorological conditions according to the Pasquill table is just checked as a diagnostic but does not weight in the model optimization), this questions the relevance of using the Gaussian plume model for such a combined inversion technique. All these problems participated to the significant errors in the statistical inversions in this study and could make such errors too large in complex cases of actual industrial emission quantification.

Therefore, while the choice of the Gaussian plume model for the initial tests to evaluate our new concept was relevant, future studies should investigate how more complex models could be integrated in this inverse modelling framework. However, the control of CFD driven dispersion models to fit the tracer data will not be straightforward even if attempting at extracting far more information from these data than simple plume indices. Even if modelling turbulent structures, the CFD models would be hardly controlled to fit that of the measurements. In general, the relevant control techniques could be

915 as complex as tracer data assimilation in these models which would make the method far more difficult
to apply than in our study. This increase of complexity may make the method quite difficult to apply
while there is a need for precise and easy-to-implement method for estimating methane emissions from
the industrial sector. From this point of view, the tracer release technique definitely appears to be the
most efficient technique.

920 Our concept faces another type of challenge. During measurement campaigns on actual industrial
sites, the locations of the methane sources are not exactly known as in our tests. This lack of information
could induce additional uncertainties to our estimates. Another source of uncertainty is the fact that in
the tested configurations, methane point sources were used whereas during field campaigns, spread and
fugitive sources may be encountered while their spatial distribution could be poorly known. The lack of
925 knowledge on the emission spatial distribution may decrease the advantage of the combined approach
(which, in its present form strongly relies on this knowledge) compared to the release technique.

At least, our experiments promotes further studies and development of our combined approach, and
even applications of our simple implementation framework to the instant quantification of the emissions
to real industrial sites for which the conditions favorable to the use of a Gaussian plume model can be
930 met.

Acknowledgement

Funding for this research was provided by Climate-KIC. The authors thank Philippe Ciais and the
industrial chair BridGES (Thales Alenia Space, Veolia, UVSQ, CEA, CNRS) for their support in this
research. We would also like to acknowledge LSCE for the permission to conduct the measurements in
935 the parking lot, particularly Pascal Doira for his availability and his help. Finally we thank the two
anonymous reviewers, L. Golston and C. Herndon, J. R. Roscioli and T. Yacovitch for their detailed and
technical comments that have helped strongly improve this study.

References

- Allen, D. T., Torres, V. M., Thomas, J., Sullivan, D. W., Harrison, M., Hendler, A., Herndon, S. C.,
940 Kolb, C. E., Fraser, M. P., Hill, A. D., Lamb, B. K., Miskimins, J., Sawyer, R. F., and Seinfeld,
J. H.: Measurements of methane emissions at natural gas production sites in the United States,
Proceedings of the National Academy of Sciences, 110, 17 768–17 773, doi:10.1073/pnas.1304880110,
URL <http://www.pnas.org/content/110/44/17768>, 2013.
- Arya, S. P.: Air Pollution Meteorology and Dispersion, Oxford University Press, 1999.
- 945 Babilotte, A., Lagier, T., Fiani, E., and Taramini, V.: Fugitive Methane Emissions from Landfills:
Field Comparison of Five Methods on a French Landfill, Journal of Environmental Engineering, 136,
777–784, doi:10.1061/(ASCE)EE.1943-7870.0000260, URL [http://dx.doi.org/10.1061/\(ASCE\)EE.1943-7870.0000260](http://dx.doi.org/10.1061/(ASCE)EE.1943-7870.0000260), 2010.
- Baklanov, A. A. and Nuterman, R. B.: Multi-scale atmospheric environment modelling for urban ar-
950 eas, Adv. Sci. Res., 3, 53–57, doi:10.5194/asr-3-53-2009, URL <http://www.adv-sci-res.net/3/53/2009/>, 2009.
- Bocquet, M.: An introduction to inverse modelling and parameter estimation for atmosphere and ocean
sciences, vol. Special Issue, pp. 461–493, 2012.
- Bort, R. and Langeron, J.: Rapport National d’Inventaire pour la France au titre de la Convention cadre
955 des Nations Unies sur les changements climatiques et du protocole de Kyoto, CITEPA, 2016.
- Brantley, H. L., Hagler, G. S. W., Kimbrough, E. S., Williams, R. W., Mukerjee, S., and Neas, L. M.: Mo-
bile air monitoring data-processing strategies and effects on spatial air pollution trends, Atmospheric
Measurement Techniques, 7, 2169–2183, doi:10.5194/amt-7-2169-2014, 2014.
- Briggs, G. A.: Diffusion estimation of small emissions, Atmospheric Turbulence and Diffusion Laboratory
960 Contribution, pp. 83–145, 1973.

- Britter, R. E. and Hanna, S. R.: Flow and Dispersion in Urban Areas, *Annual Review of Fluid Mechanics*, 35, 469–496, doi:10.1146/annurev.fluid.35.101101.161147, URL <http://dx.doi.org/10.1146/annurev.fluid.35.101101.161147>, 2003.
- Bréon, F. M., Broquet, G., Puygrenier, V., Chevallier, F., Xueref-Remy, I., Ramonet, M., Dieudonné, E., Lopez, M., Schmidt, M., Perrussel, O., and Ciais, P.: An attempt at estimating Paris area CO₂ emissions from atmospheric concentration measurements, *Atmos. Chem. Phys.*, 15, 1707–1724, doi:10.5194/acp-15-1707-2015, URL <http://www.atmos-chem-phys.net/15/1707/2015/>, 2015.
- Chevallier, F., Bréon, F.-M., and Rayner, P. J.: Contribution of the Orbiting Carbon Observatory to the estimation of CO₂ sources and sinks: Theoretical study in a variational data assimilation framework, *Journal of Geophysical Research: Atmospheres*, 112, D09 307, doi:10.1029/2006JD007375, URL <http://onlinelibrary.wiley.com/doi/10.1029/2006JD007375/abstract>, 2007.
- Czepiel, P. M., Mosher, B., Harriss, R. C., Shorter, J. H., McManus, J. B., Kolb, C. E., Allwine, E., and Lamb, B. K.: Landfill methane emissions measured by enclosure and atmospheric tracer methods, *Journal of Geophysical Research: Atmospheres*, 101, 16 711–16 719, doi:10.1029/96JD00864, URL <http://onlinelibrary.wiley.com/doi/10.1029/96JD00864/abstract>, 1996.
- Desroziers, G. and Ivanov, S.: Diagnosis and adaptive tuning of observation-error parameters in a variational assimilation, *Quarterly Journal of the Royal Meteorological Society*, 127, 1433–1452, doi:10.1002/qj.49712757417, 2001.
- Desroziers, G., Berre, L., Chapnik, B., and Poli, P.: Diagnosis of observation, background and analysis-error statistics in observation space, *Quarterly Journal of the Royal Meteorological Society*, 131, 3385–3396, doi:10.1256/qj.05.108, URL <http://onlinelibrary.wiley.com/doi/10.1256/qj.05.108/abstract>, 2005.
- Doury, A.: Une méthode de calcul pratique et générale pour la prévision des pollutions véhiculées par l’atmosphère, Rapport CEA-R-4280, 1976.
- Goetz, J. D., Floerchinger, C., Fortner, E. C., Wormhoudt, J., Massoli, P., Knighton, W. B., Herndon, S. C., Kolb, C. E., Knipping, E., Shaw, S. L., and DeCarlo, P. F.: Atmospheric Emission Characterization of Marcellus Shale Natural Gas Development Sites, *Environmental Science & Technology*, 49, 7012–7020, doi:10.1021/acs.est.5b00452, URL <http://dx.doi.org/10.1021/acs.est.5b00452>, 2015.
- Goyal, A., Small, M. J., von Stackelberg, K., Burmistrov, D., and Jones, N.: Estimation of Fugitive Lead Emission Rates from Secondary Lead Facilities using Hierarchical Bayesian Models, *Environmental Science & Technology*, 39, 4929–4937, doi:10.1021/es035465e, 2005.
- Griffith, D. W. T., Bryant, G. R., Hsu, D., and Reisinger, A. R.: Methane Emissions from Free-Ranging Cattle: Comparison of Tracer and Integrated Horizontal Flux Techniques, *Journal of Environment Quality*, 37, 582, doi:10.2134/jeq2006.0426, URL <https://www.agronomy.org/publications/jeq/abstracts/37/2/582>, 2008.
- Gurney, K. R., Law, R. M., Denning, A. S., Rayner, P. J., Baker, D., Bousquet, P., Bruhwiler, L., Chen, Y.-H., Ciais, P., Fan, S., Fung, I. Y., Gloor, M., Heimann, M., Higuchi, K., John, J., Kowalczyk, E., Maki, T., Maksyutov, S., Peylin, P., Prather, M., Pak, B. C., Sarmiento, J., Taguchi, S., Takahashi, T., and Yuen, C.-W.: TransCom 3 CO₂ inversion intercomparison: 1. Annual mean control results and sensitivity to transport and prior flux information, *Tellus B*, 55, 555–579, doi:10.1034/j.1600-0889.2003.00049.x, URL <http://onlinelibrary.wiley.com/doi/10.1034/j.1600-0889.2003.00049.x/abstract>, 2003.
- Hanna, S., White, J., Trolrier, J., Vernet, R., Brown, M., Gowardhan, A., Kaplan, H., Alexander, Y., Moussaifir, J., Wang, Y., Williamson, C., Hannan, J., and Hendrick, E.: Comparisons of JU2003 observations with four diagnostic urban wind flow and Lagrangian particle dispersion models, *Atmospheric Environment*, 45, 4073–4081, doi:10.1016/j.atmosenv.2011.03.058, URL <http://www.sciencedirect.com/science/article/pii/S1352231011003293>, 2011.

- 1010 IPCC: Climate Change 2013: The physical Science Basis. Contribution of Working Group I to the Fifth Assessment Report of the Intergovernmental Panel on Climate Change, Cambridge University Press, Cambridge, United Kingdom and New York, NY, USA, 2013.
- Korsakissok, I. and Mallet, V.: Comparative Study of Gaussian Dispersion Formulas within the Polyphemus Platform: Evaluation with Prairie Grass and Kincaid Experiments, *Journal of Applied Meteorology and Climatology*, 48, 2459–2473, doi:10.1175/2009JAMC2160.1, URL <http://journals.ametsoc.org/doi/abs/10.1175/2009JAMC2160.1>, 2009.
- 1015 Kuppel, S., Chevallier, F., and Peylin, P.: Quantifying the model structural error in carbon cycle data assimilation systems, *Geosci. Model Dev.*, 6, 45–55, doi:10.5194/gmd-6-45-2013, 2013.
- Lamb, B., Westberg, H., and Allwine, G.: Isoprene emission fluxes determined by an atmospheric tracer technique, *Atmospheric Environment (1967)*, 20, 1–8, doi:10.1016/0004-6981(86)90201-5, 1986.
- 1020 Lamb, B. K., McManus, J. B., Shorter, J. H., Kolb, C. E., Mosher, B., Harriss, R. C., Allwine, E., Blaha, D., Howard, T., Guenther, A., Lott, R. A., Siverson, R., Westburg, H., and Zimmerman, P.: Development of Atmospheric Tracer Methods To Measure Methane Emissions from Natural Gas Facilities and Urban Areas, *Environmental Science & Technology*, 29, 1468–1479, doi:10.1021/es00006a007, URL <http://dx.doi.org/10.1021/es00006a007>, 1995.
- 1025 Letzel, M. O., Krane, M., and Raasch, S.: High resolution urban large-eddy simulation studies from street canyon to neighbourhood scale, *Atmospheric Environment*, 42, 8770–8784, doi:10.1016/j.atmosenv.2008.08.001, URL <http://www.sciencedirect.com/science/article/pii/S1352231008007036>, 2008.
- Logan, J. A., Prather, M. J., Wofsy, S. C., and McElroy, M. B.: Tropospheric chemistry: A global perspective, *Journal of Geophysical Research: Oceans*, 86, 7210–7254, doi:10.1029/JC086iC08p07210, URL <http://onlinelibrary.wiley.com/doi/10.1029/JC086iC08p07210/abstract>, 1981.
- 1030 Lushi, E. and Stockie, J. M.: An inverse Gaussian plume approach for estimating atmospheric pollutant emissions from multiple point sources, *Atmospheric Environment*, 44, 1097–1107, doi:10.1016/j.atmosenv.2009.11.039, URL <http://www.sciencedirect.com/science/article/pii/S1352231009009935>, 2010.
- 1035 Mallet, V., Quélo, D., Sportisse, B., Ahmed de Biasi, M., Debry, ., Korsakissok, I., Wu, L., Roustan, Y., Sartellet, K., Tombette, M., and Foudhil, H.: Technical Note: The air quality modeling system Polyphemus, *Atmos. Chem. Phys.*, 7, 5479–5487, doi:10.5194/acp-7-5479-2007, 2007.
- Marik, T. and Levin, I.: A new tracer experiment to estimate the methane emissions from a dairy cow shed using sulfur hexafluoride (SF₆), *Global Biogeochemical Cycles*, 10, 413–418, doi:10.1029/96GB01456, URL <http://onlinelibrary.wiley.com/doi/10.1029/96GB01456/abstract>, 1996.
- 1040 Möllmann-Coers, M., Klemp, D., Mannschreck, K., and Slemr, F.: Determination of anthropogenic emissions in the Augsburg area by the source–tracer–ratio method, *Atmospheric Environment*, 36, Supplement 1, 95–107, doi:10.1016/S1352-2310(02)00212-1, URL <http://www.sciencedirect.com/science/article/pii/S1352231002002121>, 2002.
- 1045 Mønster, J. G., Samuelsson, J., Kjeldsen, P., Rella, C. W., and Scheutz, C.: Quantifying methane emission from fugitive sources by combining tracer release and downwind measurements – A sensitivity analysis based on multiple field surveys, *Waste Management*, 34, 1416–1428, doi:10.1016/j.wasman.2014.03.025, 2014.
- 1050 Pasquill, F.: Estimation of the dispersion of windborne material, *Meteor. Mag.*, 90, 33–49, 1961.
- Rayner, P. J., Enting, I. G., and Trudinger, C. M.: Optimizing the CO₂ observing network for constraining sources and sinks, *Tellus B*, 48, 433–444, doi:10.1034/j.1600-0889.1996.t01-3-00003.x, URL <http://onlinelibrary.wiley.com/doi/10.1034/j.1600-0889.1996.t01-3-00003.x/abstract>, 1996.

- 1055 Roscioli, J. R., Yacovitch, T. I., Floerchinger, C., Mitchell, A. L., Tkacik, D. S., Subramanian, R.,
Martinez, D. M., Vaughn, T. L., Williams, L., Zimmerle, D., Robinson, A. L., Herndon, S. C., and
Marchese, A. J.: Measurements of methane emissions from natural gas gathering facilities and process-
ing plants: measurement methods, *Atmos. Meas. Tech.*, 8, 2017–2035, doi:10.5194/amt-8-2017-2015,
URL <http://www.atmos-meas-tech.net/8/2017/2015/>, 2015.
- 1060 Saunois, M., Bousquet, P., Poulter, B., Peregón, A., Ciais, P., Canadell, J. G., Dlugokencky, E. J., Etiope,
G., Bastviken, D., Houweling, S., Janssens-Maenhout, G., Tubiello, F. N., Castaldi, S., Jackson, R. B.,
Alexe, M., Arora, V. K., Beerling, D. J., Bergamaschi, P., Blake, D. R., Brailsford, G., Brovkin, V.,
Bruhwiler, L., Crevoisier, C., Crill, P., Curry, C., Frankenberg, C., Gedney, N., Höglund-Isaksson, L.,
Ishizawa, M., Ito, A., Joos, F., Kim, H.-S., Kleinen, T., Krummel, P., Lamarque, J.-F., Langenfelds,
R., Locatelli, R., Machida, T., Maksyutov, S., McDonald, K. C., Marshall, J., Melton, J. R., Morino,
1065 I., O’Doherty, S., Parmentier, F.-J. W., Patra, P. K., Peng, C., Peng, S., Peters, G. P., Pison,
I., Prigent, C., Prinn, R., Ramonet, M., Riley, W. J., Saito, M., Schroeder, R., Simpson, I. J., Spahni,
R., Steele, P., Takizawa, A., Thornton, B. F., Tian, H., Tohjima, Y., Viovy, N., Voulgarakis, A., van
Weele, M., van der Werf, G., Weiss, R., Wiedinmyer, C., Wilton, D. J., Wiltshire, A., Worthy, D.,
Wunch, D. B., Xu, X., Yoshida, Y., Zhang, B., Zhang, Z., and Zhu, Q.: The Global Methane Budget:
1070 2000–2012, *Earth System Science Data Discussions*, pp. 1–79, doi:10.5194/essd-2016-25, 2016.
- Tarantola, A.: *Inverse Problem Theory and Methods for Model Parameter Estimation*, SIAM, google-
Books-ID: qLSv6fpeMowC, 2005.
- Van Poppel, M., Peters, J., and Bleux, N.: Methodology for setup and data processing of mobile air qual-
ity measurements to assess the spatial variability of concentrations in urban environments, *Environ-*
1075 *mental Pollution*, 183, 224–233, doi:10.1016/j.envpol.2013.02.020, URL <http://www.sciencedirect.com/science/article/pii/S0269749113000961>, 2013.
- Whitby, R. A. and Altwicker, E. R.: Acetylene in the atmosphere: sources, representative ambient
concentrations and ratios to other hydrocarbons, *Atmospheric Environment*, 12, 1289–1296, 1977.
- 1080 Wu, L., Bocquet, M., Chevallier, F., Lauvaux, T., and Davis, K.: Hyperparameter estimation for uncer-
tainty quantification in mesoscale carbon dioxide inversions, *Tellus B*, 65, doi:10.3402/tellusb.v65i0.
20894, 2013.
- Yver Kwok, C. E., Müller, D., Caldow, C., Lebègue, B., Mønster, J. G., Rella, C. W., Scheutz, C.,
Schmidt, M., Ramonet, M., Warneke, T., Broquet, G., and Ciais, P.: Methane emission estimates
1085 using chamber and tracer release experiments for a municipal waste water treatment plant, *Atmos.*
Meas. Tech., 8, 2853–2867, doi:10.5194/amt-8-2853-2015, URL <http://www.atmos-meas-tech.net/8/2853/2015/>, 2015.

Table 1 – Weather conditions during the four tests and configuration of the observation vector for the statistical inversion.

| Trace gas configuration | Weather conditions (avg.) | | | Total number of transects | Number of selected transects | Configuration of the observation vector for the statistical inversion |
|-------------------------|---------------------------|----------------|---------------------------------|---------------------------|------------------------------|---|
| | Temperature (°C) | Wind direction | Wind speed (m.s ⁻¹) | | | |
| Configuration 1 | 9.9 ± 0.3 | N | 3.2 ± 0.6 | 29 | 11 | Integration of the entire plume |
| Configuration 2 | 9.2 ± 0.1 | N | 3.7 ± 0.8 | 20 | 9 | Integration of the entire plume |
| Configuration 3 | 8.4 ± 0.8 | N | 2.5 ± 0.7 | 35 | 10 | Integration of the entire plume |
| Configuration 4 | 11.3 ± 0.3 | NE | 2.0 ± 0.7 | 40 | 8 | Integration of slices of the plume |

Table 2 – Methane emission rates of the different controlled release configurations estimated with the different approaches and methane fluxes actually emitted during these tests. The uncertainties given with the tracer release method are detailed as follows: standard deviation of the random uncertainty derived from the variability of the results from one transect to the other one (bias due to the mislocation of the tracer ; total uncertainty).

| | Configuration 1 | Configuration 2 | Configuration 3 | Configuration 4 |
|---|-------------------|-----------------------|--------------------|-----------------------|
| Controlled methane release (g.h ⁻¹) | 382 ± 7 | 428 ± 7 | 360 ± 7 | 482 ± 7 |
| Tracer release method estimates (g.h ⁻¹) | 434 ± 23 (0 ; 23) | 564 ± 120 (295 ; 415) | 321 ± 51 (43 ; 94) | 804 ± 160 (270 ; 430) |
| Relative difference to the control release (%) | 14 | 32 | 11 | 67 |
| Combined approach estimates (g.h ⁻¹) | 441 ± 6 | 358 ± 2 | 386 ± 2 | 462 ± 34 |
| Relative difference to the control release (%) | 15 | 16 | 7 | 4 |

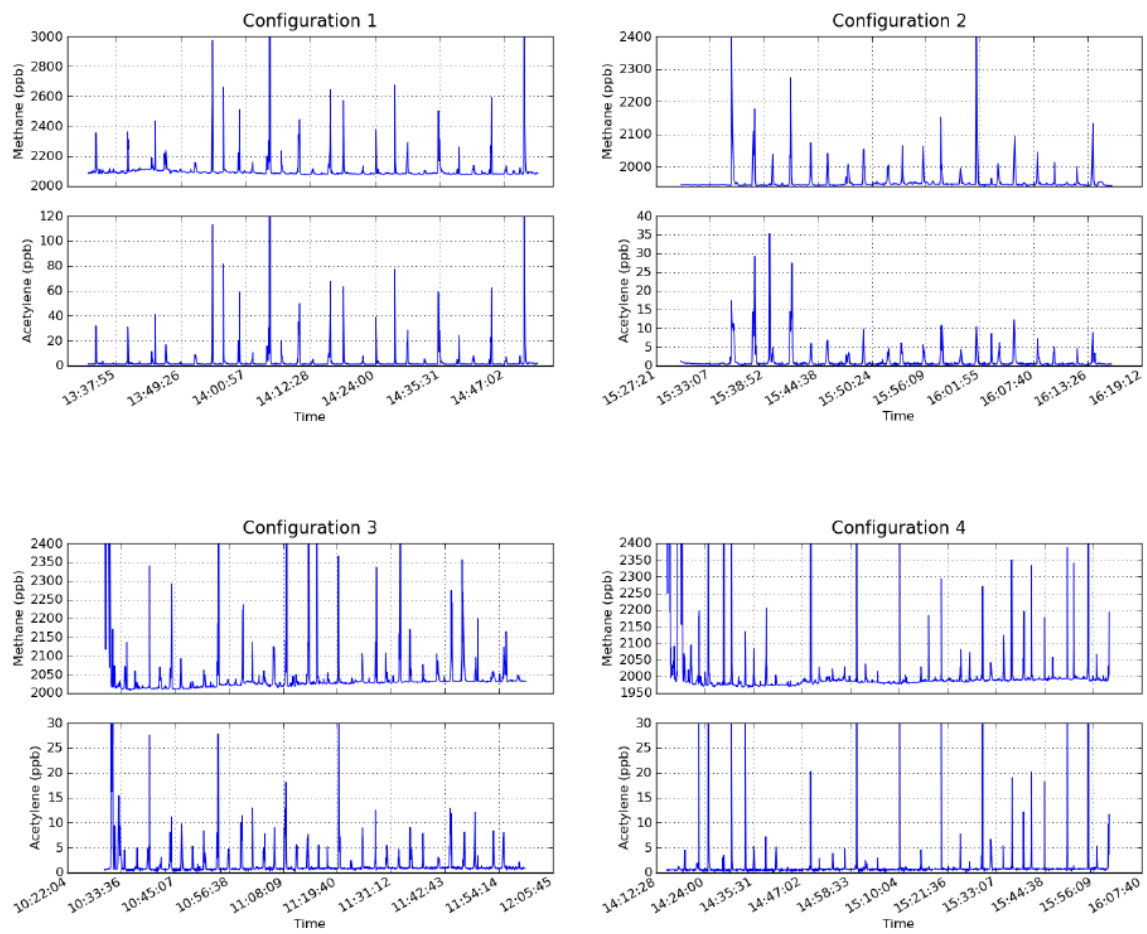


Figure 1 – Concentrations of methane and acetylene during the four tracer release experiments.



Figure 2 – The four tracer release configurations tested. Triangles represent the tracer source locations, and the circles mark methane sources. Each colour represents a configuration: blue is configuration 1, red is configuration 2, green is configuration 3 and, grey is configuration 4.

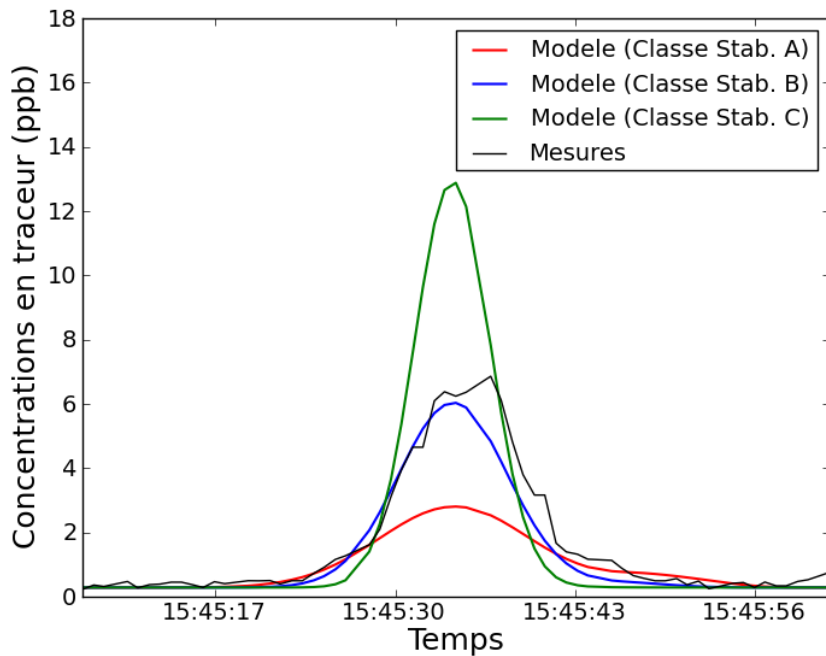
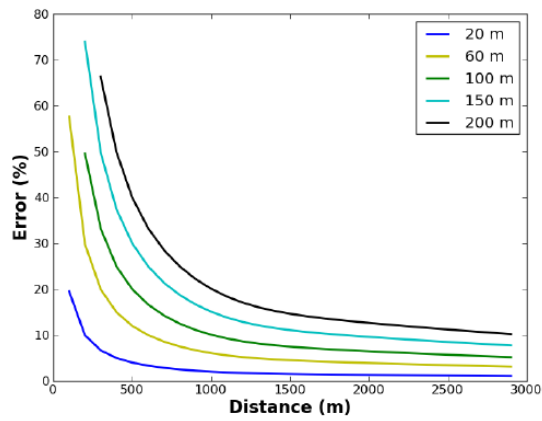
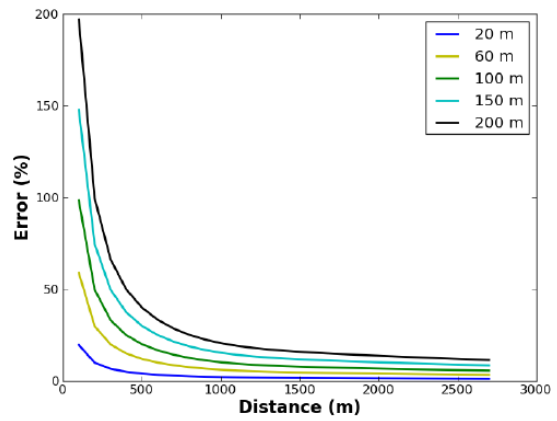


Figure 3 – Example of the Briggs parameterization selection with the acetylene data for peak 5 of configuration 2. The measured concentrations are presented in black, and the modelled concentrations with different stability classes are shown in colors.



(a) Downwind tracer shift



(b) Upwind tracer shift

Figure 4 – Error in plume estimation with the tracer method depending on the measurement distance to the methane source and a shift of 20, 60, 100 150 and 200 m of the tracer location relative to the methane source using our Gaussian plume model.

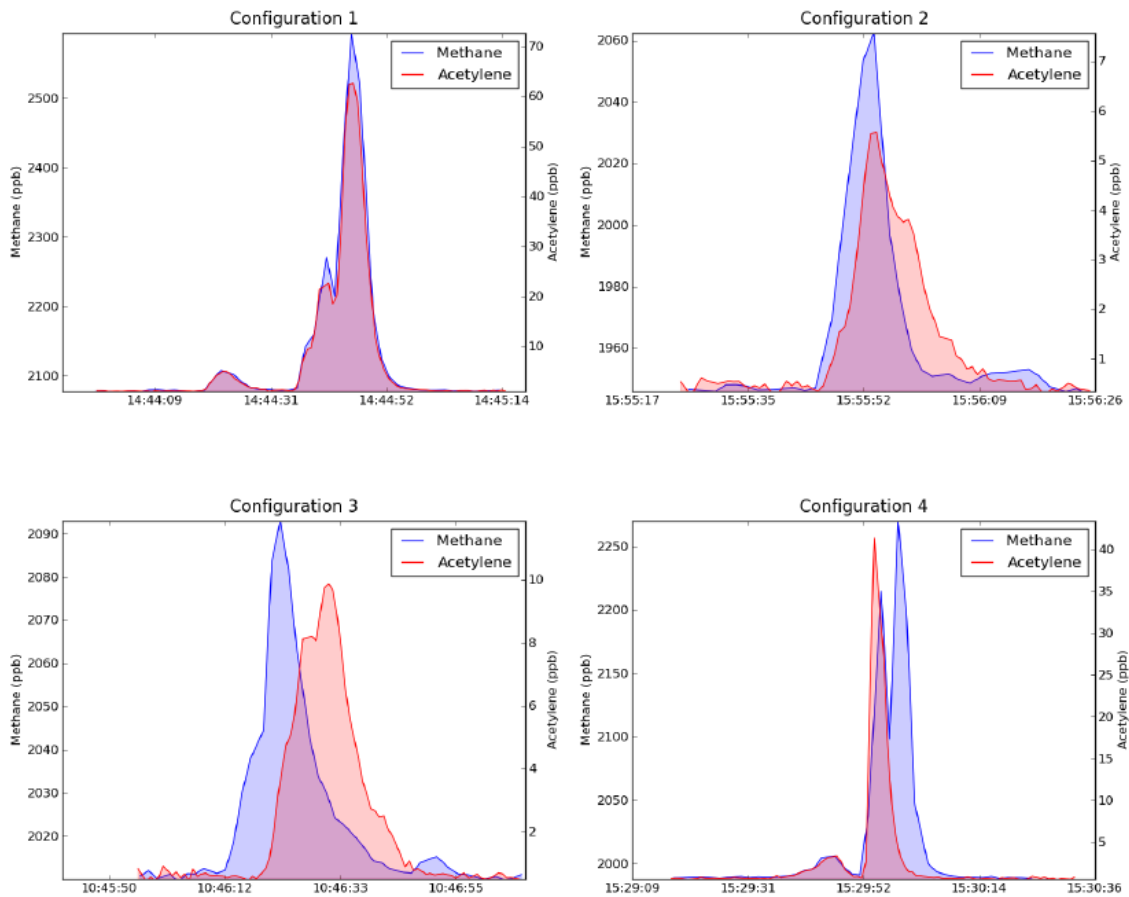


Figure 5 – Examples of cross-sections of the measured emission plumes of acetylene and methane (in red and blue, respectively) for each configuration.

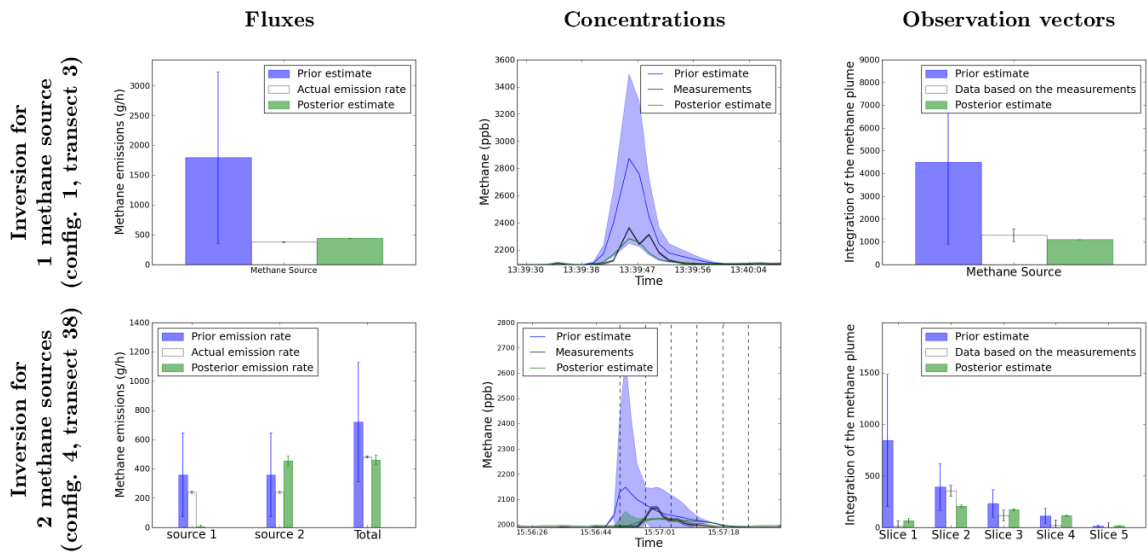


Figure 6 – Examples of prior, posterior and measured values of emission rates, concentrations and values of the observation vector for cases in configuration 1 and 4 (observations from a single transect shown).